ACS OMEGA

http://pubs.acs.org/journal/acsodf
Article

Determination of Site-Specific Phosphorylation Occupancy Using Targeted Mass Spectrometry Reveals the Regulation of Human Apical Bile Acid Transporter, ASBT

Thao T. Nguyen, Maureen A. Kane,* and Peter W. Swaan*

Cite This: ACS Omega 2024, 9, 38477−38489
Read Online

ABSTRACT: The human apical bile acid transporter (hASBT, SLC10A2) reabsorbs bile acids in the distal ileum, facilitating their recycling to the liver and resecretion. Its activity has been implicated in various disease states, including Crohn's disease, hypercholesterolemia, cholestasis, and type-2 diabetes. Post-translational modifications such as *N*-glycosylation, ubiquitination, and *S*-acylation regulate ASBT function by controlling its translocation and stability. However, the precise role of phosphorylation and its relationship with activity remains unknown. Here, we employed parallel reaction monitoring targeted mass spectrometry to investigate ASBT phosphorylation in the presence of various kinase inhibitors and activators. Our study ascertains phosphorylation at multiple sites (Thr330, Ser334, and Ser335), with Ser335 being the predominant phosphosite. We further demonstrate the critical involvement of PKC in regulating ASBT activity by phosphorylation at Ser335. Importantly, we establish a proportional relationship between the phosphorylation level of Ser335 and ASBT bile acid uptake activity. Collectively, our findings shed light on the molecular mechanisms underlying phosphorylation-mediated regulation of ASBT.

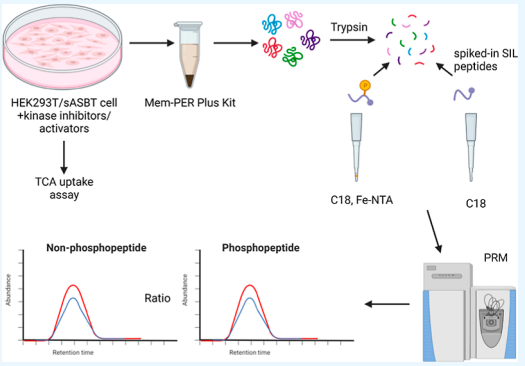

INTRODUCTION

ASBT (or SLC10A2) is a sodium-dependent bile acid transporter consisting of 348 amino acids with multipass transmembrane domains, an extracellular *N*-glycosylated amino terminus, and a cytosolic carboxyl terminus. ASBT actively transports bile acids and is primarily expressed on the apical membrane of the ileocyte; further, it has appreciable expression in kidney proximal tubule cells and cholangiocytes that line the bile duct.[1,2] After secretion in the gut from the gall bladder, ASBT is responsible for more than 90% of bile acid reabsorption to the liver where it is resecreted, resulting in only minimal loss of bile acids in urine and feces. Bile acids are synthesized from cholesterol in the liver, and this process represents a major route for the elimination of cholesterol from the body. Therefore, proper functioning of the ASBT is crucial for maintenance of the bile acid pool and cholesterol homeostasis. ASBT is thus linked to the etiology and treatment of multiple disease states, most notably hepatobiliary diseases, inflammatory bowel diseases, and metabolic diseases.[3−7] Extensive research has identified various transcription factors and nuclear receptors involved in regulation of ASBT expression at the transcriptional level. For example, transcription factor HNF1-α and CDX1/2 activate the expression of ASBT whereas GATA4 inhibits ASBT expression. Nuclear receptors such as retinoid receptor (RXR) and glucocorticoid receptor activate the expression of ASBT.[6]

At the post-transcriptional level, association with lipid rafts is important for the activity of ASBT. A study showed that disruption of lipid rafts by depleting plasma membrane cholesterol with methyl-β-cyclodextrin reduces the J_{max} of ASBT activity without affecting the amount of ASBT protein expression at the cell surface.[8] Numerous properties of ASBT such as bile acid transport, protein stability, and cell surface expression are all influenced by post-translational modifications (PTMs) such as glycosylation, ubiquitination, and palmitoylation. Recent publications show that ASBT is *S*-acylated mainly at Cys314 and inhibition of this PTM reduces ASBT uptake activity by lowering its expression on the cell surface.[9,10] ASBT has one *N*-glycosylation site at Asn10, and this modification has been shown to increase the ASBT half-life by protecting the protein from digestion by external proteases. Inhibiting glycosylation by treating cells with tunicamycin reduces ASBT activity and its expression on the plasma membrane. However, glycosylation is not required for trafficking of ASBT to the cell surface since the glycosyla-

Received: March 28, 2024
Revised: August 6, 2024
Accepted: August 7, 2024
Published: August 30, 2024

tion-deficient mutant N10E has the same rate of trafficking to the plasma membrane as fully glycosylated wildtype ASBT.[11,12] ASBT is degraded via ubiquitination, and rat Asbt has a short half-life of about 6 h. Analysis of protein turnover revealed that the double mutation of two potential phosphosites Ser 335/Thr339 to Ala prolonged ASBT half-life and rendered this mutant resistant to IL1β-induced proteasome degradation of ASBT.[13] This study, therefore, suggested that phosphorylation may be required for the IL1β-mediated degradation of ASBT.

Multiple lines of evidence suggest that ASBT is regulated by kinase(s), but their exact mechanism of action has not yet been elucidated. Protein kinase C (PKC), protein kinase A (PKA), MEK1/2, MAP kinase, and tyrosine kinase have all been implicated in the regulation of bile acid transport. Inhibition of MEK1/2 and p38 MAP kinase results in a decrease in the activity of ASBT in freshly isolated rat kidney tubular cells. Schlattjan and colleagues showed that increasing cellular levels of cAMP, a known activator of PKA, with forskolin, 3-isobutyl-1-methylxanthine (IBMX), or 8-Br-cAMP inhibited ASBT uptake activity.[14] Analogously, Sarwar and co-workers suggest a functional role for PKC in ASBT regulation since treatment of Caco2 cells transiently expressing ASBT with PKC activators reduced its plasma membrane expression and uptake activity.[15] Recent studies have also suggested ASBT is phosphorylated at tyrosine residues[16] and treatment with a tyrosine phosphatase inhibitor was shown to prevent the negative effect of enteropathogenic *Escherichia coli* (EPEC) on ASBT function.[17] Inhibition of protein tyrosine phosphatase both increased ASBT uptake activity and its protein expression at the plasma membrane, suggesting a role for tyrosine phosphorylation in ASBT activation. In addition, adverse effects were observed when these cells were treated with an inhibitor of tyrosine Src family kinases, suggesting that tyrosine phosphorylation increases ASBT's cell surface expression and function.[18] Notably, there appear to be conflicting data in these studies because both kinase inhibitors and activators inhibit ASBT function, and no studies directly demonstrate the effect of kinase inhibitors or activators on ASBT phosphorylation, likely due to the lack of a specific ASBT phosphoantibody. Another major challenge in the characterization of kinase effects is identifying the underlying mechanisms and determining whether actions are mediated by the phosphorylation of the ASBT protein itself, the phosphorylation of other ASBT-associated proteins, or a combination of the two.

In this study, we used targeted mass spectrometry to investigate ASBT phosphorylation and the underlying mechanism of both kinase inhibitors and activators for ASBT phosphorylation and its resulting activity. Until now, mass spectrometry-based characterization of ASBT phosphorylation had not been reported, likely due to the low abundance of plasma membrane proteins in global phosphoproteomics,[19] which typically uses data-dependent acquisition (DDA) methodology. DDA mass spectrometry excels at sampling the most abundant precursor ions for further fragmentation, but this comes at the expense of the less abundant precursor ions (such as phosphopeptides from integral plasma membrane proteins) and, therefore, can exclude important biological information. Furthermore, phosphorylation is usually highly dynamic with low stoichiometries, making it more difficult to identify and quantify the phosphorylation of membrane proteins in general. Over the years, the development of targeted mass spectrometry techniques, such as selected reaction monitoring (SRM) has improved the detection and quantification of low abundance proteins and PTMs in complex mixtures. SRM is usually performed in a tandem quadrupole (QqQ), with Q1 and Q3 selectively filtering individual precursor and product ion transitions using narrow isolation windows in tandem. As a result, SRM significantly increases selectivity, and sensitivity is increased by one to 2 orders of magnitude when compared to traditional DDA.[20] Parallel reaction monitoring (PRM) is similar to SRM in that it isolates a target precursor, which is then fragmented, and all of the product ions are detected in parallel.[21,22] With the recent introduction of PRM on a number of instrument platforms including quadrupole-Orbitrap (e.g., Thermo Q-Exactive), quadrupole-Orbitrap-linear ion trap (e.g., Thermo Fusion Tribrid), and hybrid quadrupole/time-of-flight (QqTOF) (e.g., Sciex Triple TOF), it is now possible to use targeted high resolution MS/MS methods to quantify low abundance proteins in complex mixtures without requiring laborious optimization of transitions chosen for traditional SRM targeted mass spectrometry workflows.[23,24] Here, we present a workflow that employs PRM mass spectrometry and stable isotope labeled peptides (SIL) to quantify the phosphorylation occupancy of ASBT in the presence and absence of various kinase inhibitors and activators. Our findings provide the first evidence of ASBT phosphorylation at three C-terminal domain residues: Ser335, Thr330, and Ser334, with Ser335 being the most abundant and (likely most) important in regulating ASBT function. Furthermore, we discovered that inhibiting Ser335 phosphorylation with a PKC kinase inhibitor decreases uptake activity, whereas treatment with a PKC kinase activator increases the ASBT phosphorylation occupancy and bile acid uptake activity, implying that PKC regulates ASBT phosphorylation. Finally, we found that PKCα is the isoform that might directly phosphorylate ASBT at Ser335 because overexpression of this isoform, but not other isoforms, increases ASBT phosphorylation. Our identification of a specific kinase that regulates ASBT protein phosphorylation and activity will aid in the future development of therapeutics that regulate transporter protein activity by directly targeting its PTM.

EXPERIMENTAL SECTION

Materials and Chemicals. [^{3}H]-Taurocholic acid (TCA) was purchased from PerkinElmer (Waltham, MA). Taurocholic acid, mouse anticalnexin, and polybrene infection were from Sigma (St. Louis, MO). Rabbit anti-ASBT was obtained from Proteintech (Rosemont, IL). Secondary antibodies were purchased from Licor (Lincoln, NE). Cell culture media and supplies, puromycin dihydrochloride, Halt Protease and Phosphatase Inhibitor Cocktail, EDTA-free (100×), Mem-PER Plus Membrane Protein Extraction Kit, and High-Select Fe-NTA Phosphopeptide enrichment kit were from Invitrogen (Carlsbad, CA). Bisindolylmaleimide I (BIM1), Forskolin, H-89 dihydrochloride, KN-93, and Phorbol 12-myristate 13-acetate (PMA) were from Calbiochem (Sigma, St. Louis, MO). CCG215022, U0126, and SB203580 were purchased from Selleck Chemicals (Houston, TX). CMPD101 was obtained from MedChemExpress (Monmouth Junction, NJ). Streptactin resin was purchased from GE Healthcare (Silver Spring, MD). Sodium dodecyl sulfate (SDS) was from Fisher (Waltham, MA). *n*-Dodecyl-β-D-maltopyranoside (DDM), Anagrade, was from Anatrace (Maumee, OH). Sequencing Grade Modified Trypsin was from Promega (Madison, WI). All other chemicals and reagents used were of the highest purity available commercially.

https://doi.org/10.1021/acsomega.4c02999
ACS Omega 2024, 9, 38477−38489

Plasmid Generation and Cell Culture. A previous construct of the pCMV-hASBT was used as the template.[10] Primers were designed using the QuikChange primer design tool (Agilent, Santa Clara, CA) and the Strep tag II and (GlyGlyGlySer)×2 repeat linker were introduced at the N-terminus of ASBT using QuikChange II Site-Directed Mutagenesis kit (Agilent, Santa Clara, CA). Strep tag II-(GlyGlyGlySer)×2-tagged ASBT (refereed as sASBT) was amplified and ligated to the pCR8-TOPO/GW plasmid (Invitrogen, Carlsbad, CA). Gateway LR Clonase (Invitrogen, Carlsbad, CA) was then used to transfer the sASBT sequence into the pLenti-CMV-Puro-DEST vector backbone (Addgene, Watertown, MA). pLenti-CMV-Puro-DEST (w118-1) was a gift from Eric Campeau and Paul Kaufman (Addgene plasmid number 17452).[25] The sequence and direction of pLenti-CMV-Puro-sASBT were confirmed by DNA sequencing. The pLenti-CMV-Puro-sASBT were used to produce Lenti-sASBT by Origene (Rockville, MD). The plasmids for expression of PKC isoforms were a gift from Alex Toker (Addgene plasmid number 10795,10799, 10805).[26−28] COS1 and human embryonic kidney-293T (HEK293T) cells were obtained from American Type Culture Collection (ATCC, Manassas, VA) and were grown routinely in T-225 plastic flasks at 37 °C in a 5% CO_2 environment. COS-1 cells (ATCC CRL-1650) and HEK293T (ATCC #70029111) were grown in DMEM with 10% FBS, 1% nonessential amino acids, and 1% penicillin/streptomycin (Complete Medium).

HEK293T cells were transduced with 5 MOI of Lenti-sASBT in the presence of 8 μg/mL polybrene to enhance the transduction efficiency. Cells expressing sASBT were selected by the addition of puromycin, and ASBT expression was verified by Western blot. Stable cell lines were obtained after selection by long-term culture in a medium containing 1 μg/mL puromycin for 14 days. Clones derived from HEK293T cells stably transfected with Lenti-sASBT were referred as HEK293T/sASBT cells. HEK293T/sASBT were routinely maintained in Complete Medium with 1 μg/mL of puromycin.

Uptake Assay and Transporter Kinetic Measurements. pCMV5-ASBT, pCMV5-sASBT were transiently expressed in COS-1 cells using Opti-MEM reduced serum medium (Life Technologies, Inc., Hunt Valley, MD) and Turbofect transfection reagent (Thermo Scientific, Waltham, MA) according to the manufacturers' directions. Briefly, COS-1 cells were seeded at 7×10^4 cells/ml in 24-well plate for TCA uptake assay. After 24 h, cells were transfected with WT or sASBT using Turbofect transfection reagent (1 μg plasmid DNA: 4 μL Turbofect) and Opti-MEM reduced serum medium. Six hours after transfection, the medium was replaced with the Complete Medium and grown for another 24 h for uptake assay. HEK293T/sASBT were seeded at 3×10^5 cells/ml in 12 well plate for up to 2 days until reaching about 85−90% confluency for TCA uptake assay. Cells were washed once with prewarmed Dulbecco's phosphate-buffered saline DPBS (containing calcium and magnesium) and then incubated at 37 °C for 12 min in Modified Hanks' balanced salt solution, pH 7.4, containing 10 μM cold nonradiolabeled TCA spiked with 1 μCi/mL [^{3}H]-TCA. The transport assay was stopped by removing the reaction buffer and washing three times with cold DPBS. Cells were lysed in 350 μL of 0.05% SDS. Radioactivity associated with cells was measured by liquid scintillation counting using Tri-Carb 2910TR (PerkinElmer, Waltham, MA). Protein concentration was quantified using the BCA assay (Thermo Scientific, Waltham, MA) and uptake rates were determined as nmol/mg total protein/min.

Substrate kinetics for sASBT stably expressed in HEK293T was analyzed by measuring the uptake with increasing concentrations of TCA (0−200 μM). The Michaelis−Menten-like constant (K_t) and maximal transport velocity (J_{max}) were determined using GraphPad 8.4 (San Diego, CA), by fitting the Michaelis−Menten equation describing a single saturable transport system to the data: $V = J_{max} \times S/(K_t + S)$ where V is the uptake rate, S is the substrate concentration, K_t is the Michaelis−Menten-like constant, and J_{max} is the maximal transport velocity.

Western Blot. Protein concentrations were measured with the BCA assay (Thermo Scientific, Waltham, MA). 25 μg of total protein extracted from HEK293T/sASBT were separated on Bolt 4−12% Bis-Tris protein gel (Invitrogen, Carlsbad, CA), then blotted on a PVDF membrane via dry transfer using the iBlot2 system (Thermo Scientific, Waltham, MA). Primary antibodies including (1)-rabbit anti-ASBT polyclonal antibody (Proteintech, Rosemont, IL), (2)-mouse anticalnexin monoclonal antibody, and (3)-mouse anti-FLAG monoclonal antibody (Sigma, St. Louis, MO) were diluted at 1:1000. Secondary antibodies, donkey anti rabbit IR 800, and donkey anti mouse IR680 (Licor, Lincoln, NE) were diluted at 1:10,000. Detection was undertaken using the Odyssey CLX imaging system (Licor, Licoln, NE) and its companion software, Image Studio.

Sample Preparation for LC−MS/MS. For proteomics analysis, HEK293T/sASBT cells were seeded at 1.3×10^6 cell/ml in a 15 cm dish and grown for 1−2 days to reach ca. 90% confluency. The cells were then treated with 0.1% DMSO as vehicle control or with the kinase inhibitors or kinase activators, all in the final concentration of 0.1% DMSO at the time of treatment in triplicates. The cells were then washed twice with cold PBS and membrane protein was enriched using Mem-PER Plus kit (Invitrogen, Carlsbad, CA) with a modified protocol as following. All of the following steps were performed at 4 °C. Briefly, the cells were washed with the cell wash solution twice, then lysed with the permeabilization buffer for 10 min, and centrifuged at 16,000*g* for 15 min. The cytosolic fraction was removed, and the total membrane pellet was solubilized with 1% DDM in 50 mM Tris pH 8.0, 150 mM NaCl, 10% glycerol with freshly added Halt Protease and Phosphatase Inhibitor Cocktail. Membrane proteins were then solubilized by rotating at 4 °C for 1 h and then centrifuged at 16,000*g* for 15 min to remove the insoluble fraction. For the initial analysis of the phosphorylation of ASBT, the solubilized membranes were diluted 4 times with 50 mM Tris, pH 8.0, 150 mM NaCl to reduce the DDM concentration to 0.25% and incubated with streptactin resin (GE Healthcare, Silver Spring, MD) for 1 h to purify sASBT. The resin was washed three times with 50 mM Tris, pH 8.0, 300 mM NaCl, 0.05% DDM and washed two times with 50 mM Tris, pH 8.0. The proteins were then denatured and reduced on resin by addition of 2 M urea and 5 mM tris(2-carboxyethyl)phosphine (TCEP) and incubated at 56 °C for 30 min with gentle vortex for every 10 min. The proteins were then alkylated with 14 mM iodoacetamide (IAA) for 30 min in the dark at room temperature after which the reaction was stopped by addition of 5 mM DTT for 15 min at room temperature in the dark. The urea was diluted to 1 M by adding 50 mM Tris, pH 8.0. The proteins were digested on resin with 0.5 μg of trypsin overnight at 37 °C in the shaker. The reaction was stopped by

https://doi.org/10.1021/acsomega.4c02999
ACS Omega 2024, 9, 38477−38489

adding 0.5% TFA and spinning at 13,000*g* for 5 min to remove any insoluble materials. The peptides were then desalted with C18 Omix tips (Agilent, Santa Clara, CA), dried by Speedvac, and used for phosphopeptide enrichment. The phosphopeptides were enriched using the High Select Phosphopeptide enrichment Kit (Invitrogen, Carlsbad, CA) according to the manufacturer's recommendations. Briefly, the peptides were resuspended in binding buffer and then loaded to the Fe-NTA spin column and incubated for 30 min at room temperature and mixed for every 10 min by gently tapping the tube. The nonphosphopeptides were then washed with the binding buffer 3 times and washed with deionized water 1 times. The phosphopeptides were eluted twice with 100 μL elution buffer each time and combined. The eluted phosphopetides were then dried immediately using SpeedVac (Thermo, Waltham, MA) and then resuspended and acidified with 0.5% formic acid (FA) and loaded to nanoLC-MS/MS.

The membrane fractions for the quantification of phosphorylation of ASBT by targeted PRM mass spectrometry were prepared as follows. The DDM-solubilized membrane fraction was precipitated using the methanol/chloroform method.[29] Proteins were then solubilized with 8 M urea in 50 mM ammonium bicarbonate buffer, 5 mM TCEP and reduced at 56 °C for 30 min and alkylated with 14 mM IAA for 30 min in the dark. Urea was diluted to 1 M final concentration before adding trypsin at 1:100 (enzyme/substrate ratio by weight) and digestion was carried out overnight at 37 °C in a shaker. Digestion was stopped by addition of 0.5% TFA. The peptide mixture was diluted two times and quantified using the Pierce Quantitative Colorimetric Peptide Assay (Thermo Scientific, Waltham, MA). A background matrix was generated by pooling aliquots of all individual samples from each batch and spiked with SIL peptides to estimate the amount of phosphopeptide and nonphosphopeptide from each batch. 150 μg peptide from each sample were spiked with an equal amount of SIL nonphosphopeptide or SIL Ser335 phosphopeptide. The SIL Ser335 phosphopeptide was spiked at 2.1−12 fmol per 1 μg total peptide whereas the SIL nonphosphopeptide was spiked at 50−300 fmol per 1 μg total peptides. After cleaning with a C18 tip, 1 μg of the fractions spiked with nonphosphopeptide SIL were directly used for mass spectrometry analysis, whereas the whole fractions spiked with SIL Ser335 phosphopeptide were further enriched with the High-Select Fe-NTA Phosphopeptide Enrichment Kit. The SIL for nonphosphopeptide and corresponding Ser335 phosphopeptide were at high purity (AQUA basic >95% purity). In contrast, the SIL standards for phosphopeptide at Ser334 and Thr330 were crude as synthesized (PEPotec grade 3; all purchased from Thermo Scientific, Waltham, MA). We hypothesized from our previous studies preliminary data that Ser335 is the main phosphorylation residue; therefore, the other two SIL phosphopeptides were used as crude phosphopeptide for the purpose of determining the coelution time to identify their endogenous phosphoisoform only.

LC−MS/MS. Samples were analyzed on a NanoACQUITY UPLC (Waters, Milford, MA) coupled with a Q Exactive HF mass spectrometer (Thermo Scientific, San Jose, CA). A nanoelectrospray ion source was utilized with stainless steel emitter (40 mm length, 150 μm outer diameter, 30 μm inner diameter, #ES542, Thermo Scientific, Waltham, MA). Spray voltage was set to 3 kV, funnel RF level was set to 70, and the capillary was heated at 275 °C. The UPLC was equipped with a trapping column (ACQUITY UPLC M-Class Symmetry C18 Trap Column, 100 Å pore size, 5 μm particle size, 180 μm by 2 cm; Waters, Milford, MA) for washing and preconcentration; and an analytical column (ACQUITY UPLC M-Class Peptide BEH C18 Column, 130 Å pore size, 1.7 μm particle size, 75 μm by 25 cm; Waters, Milford, MA) for separation of the peptides. Preconcentration was performed for 10 min at a flow rate of 15 μL/min using 0.1% FA in water, and separation was performed at a flow rate of 200 nL/min. The column was kept at 45 °C. A binary gradient of solvent A (0.1% FA in water) and B (0.1% FA in 100% acetonitrile) was used with the following steps: 0 min, 3% B, 1 min, 3% B; 2 min, 15% B; 60 min, 30% B; 70 min, 45% B; 75 min, 100% B; 85 min, 100% B; 86 min, 3% B; 96 min, 3% B. For analysis in data dependent mode (DDA), full scan MS spectra (m/z 300−1500) in profile mode were acquired in the Orbitrap with a resolution of 60,000, automatic gain control (AGC) value of 3×10^6, and maximum fill times of 200 ms. The top 15 peptide signals (charge state 2^+ to 6^+) were isolated (1.4 m/z window) and fragmented by higher energy collision (HCD), normalized collision energy (NCE) of 28.0 and measured in the Orbitrap with an AGC target of 5×10^4 and a resolution of 15,000, and maximum fill time of 50 ms for the MS/MS scans. For the analysis of the stable isotope-labeled peptides in membrane protein fraction for nonphosphopeptide and phosphopeptide of ASBT, the acquisition method combined a full scan method with multiplexed PRM method analysis. We did not schedule the acquisition time because each run only had a pair of endogenous and SIL peptides but instead collected data from 15 to 30 min of 96 min gradient based on preliminary data for retention time of ASBT's peptides. The Full MS-SIM method employed an m/z 300−1500 mass selection, an Orbitrap resolution of 60,000, target AGC AGC values of 3×10^6, and maximum fill times of 250 ms. For PRM mode, a resolution of 30,000 with a fixed first mass of 120 m/z. The AGC target was set to 1×10^6 and a maximum injection time of 125 ms. Targeted precursors were isolated with a quadrupole isolation width of 2.0 m/z for phosphopeptide and 0.4 m/z for nonphosphopeptide and fragmented with a NCE of 28.

Data Analysis. Raw files from DDA and PRM analyses were processed using Proteome Discoverer 2.5 and searched against UniProt *Homo sapiens* database; 20, 194 sequences (concatenated with the reverse database). For the database search, the following settings were used: trypsin was set as the proteolytic enzyme with a maximum of two missed cleavages; oxidation of methionine and phosphorylation of serine, threonine, and tyrosine were set as variable modifications; and cysteine carbamidomethylation was set as a fixed modification. A peptide mass tolerance of 10 ppm and a fragment mass tolerance of 0.05 Da were allowed. Peptides were identified with a false discovery rate of 1% as a confidence threshold based on a concatenated decoy database search. Phosphosite assignments were searched with the IMP-ptmRS node in Proteome Discoverer with a site probability threshold of 75%.

Skyline Software (ver. 20.1)[30] was used to quantify the amount of nonphosphopeptide and Ser335 phosphopeptide from the PRM data. The top three to five most suitable transitions of every light and SIL peptide pair were chosen. All data were manually inspected for correct peak assignment, retention time, and integration, and amount of peptide were exported for further analysis. GraphPad Prism (version 8.4, San Diego, CA) was used for statistical analysis. The phosphorylation occupancy was calculated using the following formula:

https://doi.org/10.1021/acsomega.4c02999
ACS Omega 2024, 9, 38477−38489

phosphorylated peptide/(phosphorylated peptide + non-phosphorylated peptide) × 100 = (%) phosphorylation.

STATISTICS

Values are presented as the mean ± standard deviation (SD). Statistically significant differences between groups were tested using Student's *t*-test for two conditions or by using repeated measures ANOVA followed by the Dunnett's comparison test for multiple comparisons (GraphPad Prism Software, Inc. version 8.4, San Diego, CA). Results were considered to be statistically significant at $p < 0.05$.

RESULTS

Model System for Phosphoproteomic Analysis of Membrane Protein ASBT. To study the phosphorylation of human ASBT by mass spectrometry, we designed a protein construct with a Strep-tag II with two Gly−Gly−Gly−Ser linkers at the N-terminus (termed hereafter as sASBT). This tag was chosen because the high purification efficiency and specificity of the Strep tag in isolating plasma membranes is well-documented in multiple studies.[33−35] At first, we used transient expression of wildtype ASBT and sASBT in COS1 cells to study the function of sASBT. The results demonstrated that the Strep-tag II has no effect on ASBT taurocholate uptake and has a similar function as the wildtype ASBT (Figure S1A). We then designed another construct of sASBT in the pLenti-CMV-puro-DEST backbone to stably express the tagged ASBT in HEK293T cells for large scale purification of ASBT for mass spectrometry-based analysis. The expression of stably expressed ASBT was confirmed by Western blot, and the HEK293T that transiently expressed the backbone empty vector was used as a negative control (Figure S1B). Furthermore, kinetic analysis of the stably expressed sASBT confirmed that sASBT has J_{max} of 0.322 ± 0.018 nmol/mg/min and K_t of 31.012 ± 5.349 μM (Figure S1C) which is consistent with what has been previously reported for wildtype ASBT.[10,18]

ASBT is Phosphorylated at Three Sites. The stably expressing sASBT cells were used for DDA and PRM-based phosphoprotein analyses to determine the sites that are phosphorylated in ASBT. To determine ASBT phosphorylation, we initially enriched the total membrane fraction, followed by purification of sASBT using streptactin resin. Subsequently, we conducted trypsin digestion of the purified sASBT on the resin and enriched for phosphopeptides. Finally, we employed a Q-Exactive HF instrument for data acquisition through a combination of DDA and PRM analysis. Figure 1 depicts the spectra of ASBT phosphorylated at three different sites, with specific b- and y-ions to differentiate these phosphorylation sites. Ser335, Thr330, and Ser334 were identified as phosphosites of ASBT.

PRM Analyses of Sample Spiked with SIL Phosphopeptide Isoforms Confirm ASBT is Phosphorylated at Three Sites, with Ser 335 Being the Most Abundant. To conduct comprehensive PRM-based phosphoproteomic analysis, we employed stably expressing sASBT cells and utilized stable isotope labeled phosphopeptides of three identified phosphosites. By employing specific stable isotope labeled phosphopeptides corresponding to each site, we were able to precisely identify the distinct phosphoisoforms of ASBT. As shown in Figure 2, three phosphoisoform peptides were eluted at three distinct peaks with each having retention times similar to those of their corresponding SIL phosphoisoform. Based on

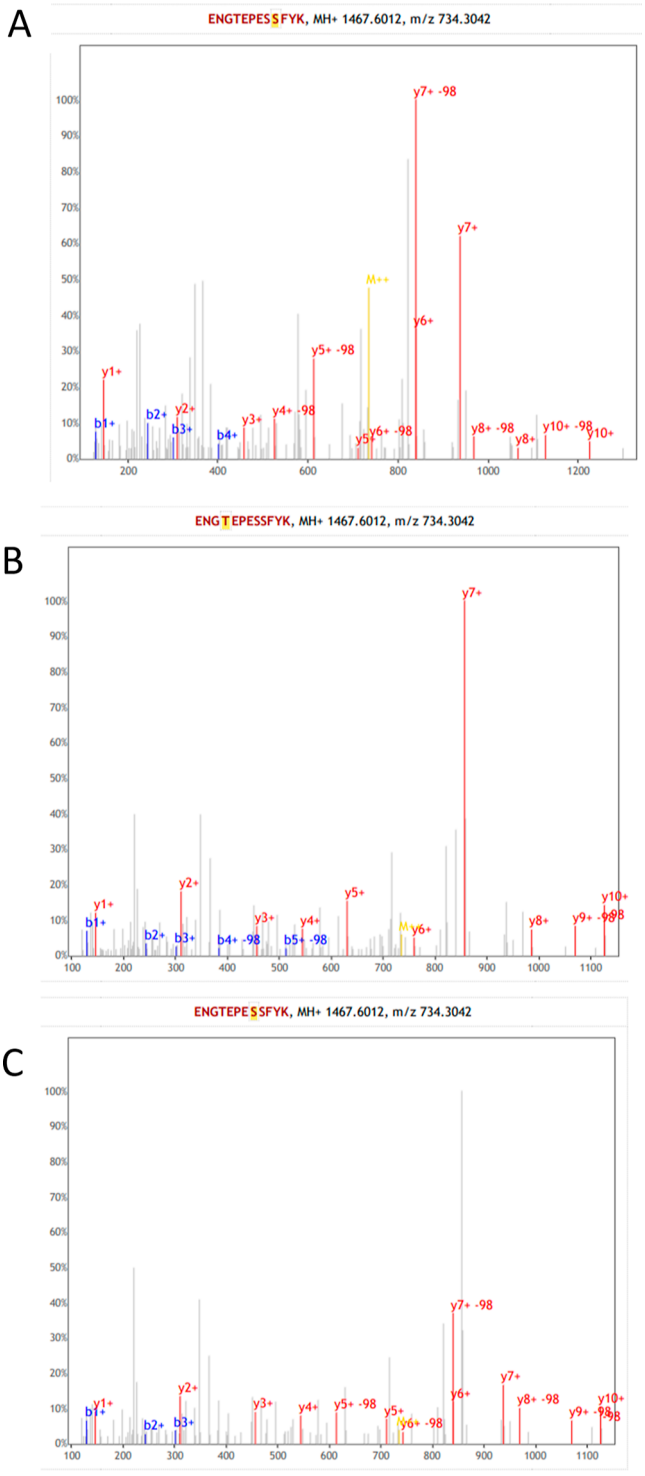

Figure 1. Diagnostic spectra identifying phosphorylation of ASBT at Ser335, Thr330, and Ser334. Phosphopeptides were enriched with an Fe-NTA spin column before being analyzed with nanoLC-MS/MS using DDA and PRM. The b- and y-ion series confirming phosphorylation of ASBT are shown for Ser335 (A), Thr330 (B), and Ser334 (C).

the coelution of the endogenous phosphpopeptides with their SIL phosphoisoforms, we were able to determine that the first and most abundant peak is phosphorylation of ASBT at Ser335, followed by peaks for the phosphorylation of Thr330 and Ser334 which had some overlap retention time and at

https://doi.org/10.1021/acsomega.4c02999
ACS Omega 2024, 9, 38477−38489

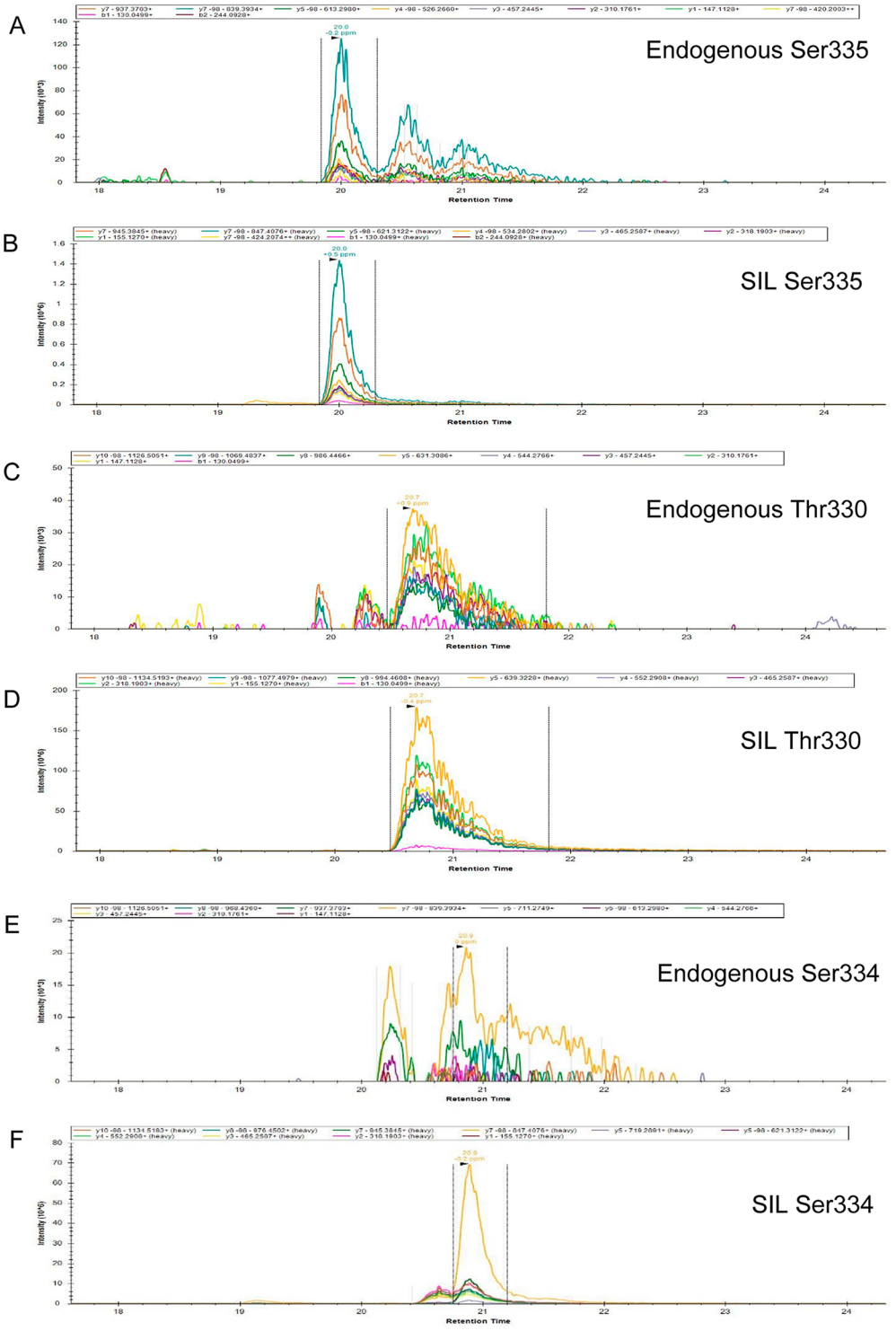

Figure 2. Targeted high-resolution MS/MS combined with spiked-in SIL phosphopeptides identifies ASBT is phosphorylated at three sites Ser335, Thr330, and Ser334 with Ser335 being the most abundant. Phosphopeptides were enriched with an Fe-NTA spin column before being analyzed with nanoLC-MS/MS using PRM. Endogenous phosphopeptides (upper panel) were coeluted with their corresponding spiked-in stable isotope-labeled phosphoisoforms (lower panel), respectively, for Ser 335 (A,B), Thr330 (C,D), and Ser 334 (E,F). The y- and b-ion series, shown at the top of each image, further confirm the phosphorylation of ASBT at these three residues.

lower intensity. Interestingly, Ser335, the most abundant phosphosite, is a conserved residue in chicken, dog, rat, mouse, hamster, rabbit, and human ASBT (Figure S2).[36] This suggests the potential for this phosphosite to regulate the ASBT function in all of these species. Due to the frequently low signal intensity of the two subsequent peaks (Thr330 and Ser334), it was challenging to achieve reliable integration of the fragment peaks in the extracted ion chromatograms. As such, we only used the SIL of Ser335 phosphopeptide to quantify ASBT phosphorylation at the Ser335 site in the following sections. The SIL nonphosphopeptide counterpart was used to quantify the nonphosphoprotein level.

https://doi.org/10.1021/acsomega.4c02999
ACS Omega 2024, 9, 38477−38489

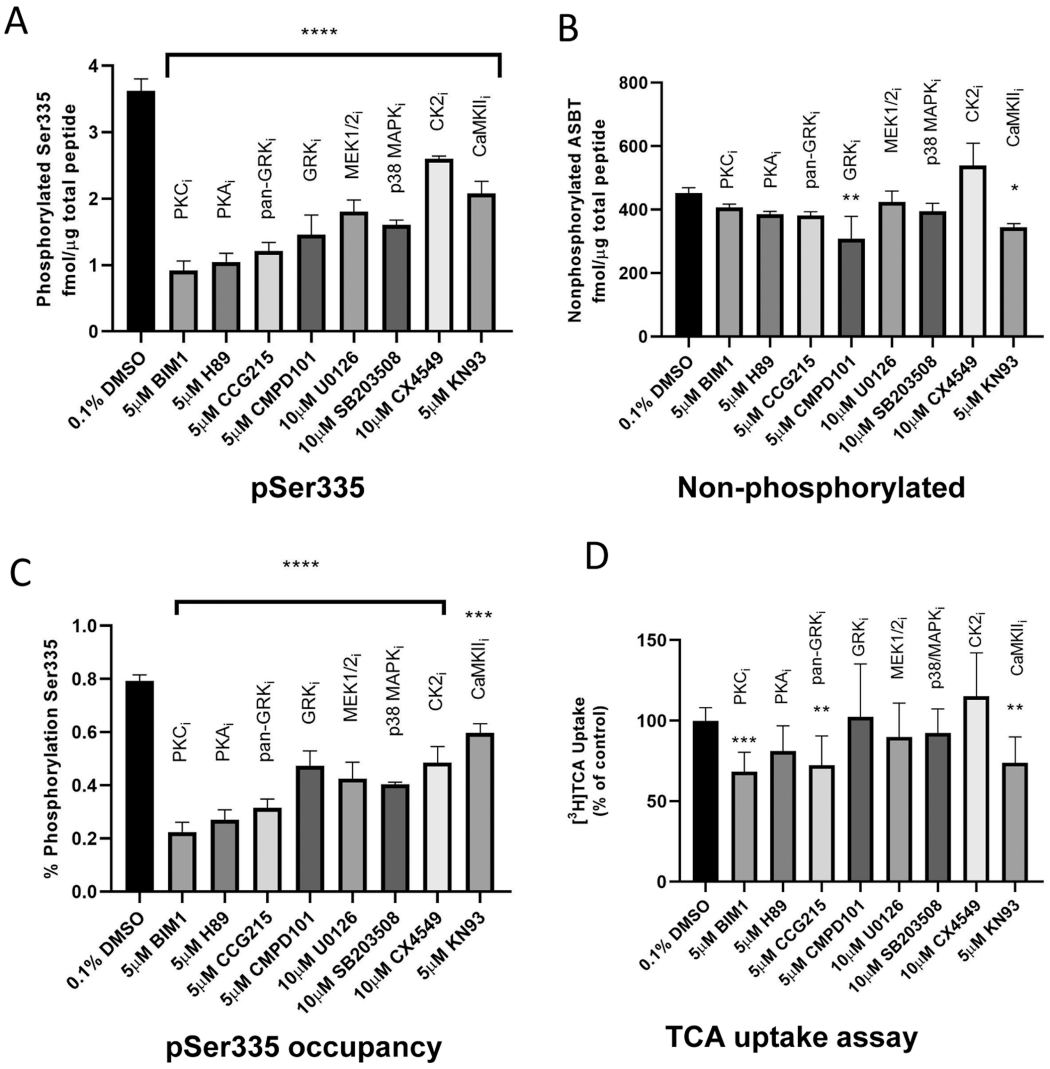

Figure 3. Quantification of phosphorylation occupancy shows kinase inhibitors inhibit ASBT phosphorylation and its TCA uptake activity. Amount of Ser 335 phosphopeptide and its nonphosphopeptide counterpart were quantified as fmol/μg total peptide based on the known amount of spiked-in stable isotope labeling peptides. Amount of phosphorylated ASBT at Ser335 (A), and its corresponding nonphosphorylated peptide (B), and Ser335 phosphorylation occupancy (C), and TCA uptake assay of ASBT after 6 h of treatment with various kinase inhibitors compared to the vehicle control DMSO. Uptake of TCA was measured in a 12 min assay using 10 μM cold nonradiolabeled TCA spiked with 1 μCi/mL [^{3}H]-TCA. Uptake assay data are presented as percentage of control. Values are mean ± SD with n = 3 for A,B,C, n = 12 for D. Significance levels are indicated as follows ****p-value <0.0001, ***p-value <0.0003, **p-value <0.006 (Dunnett's post hoc test), indicating statistical significance compared to the control.

Using PRM to Quantify Phosphorylation Occupancy Shows Kinase Inhibitors Inhibit Ser335 Phosphorylation and ASBT Function. To quantify the occupancy of Ser335 phosphorylation and elucidate the kinase involved in the regulation of ASBT phosphorylation at this specific site, we implemented a targeted mass spectrometry PRM method. The experimental strategy involved treating cells with various kinase inhibitors, followed by quantification of the phosphorylation ratio at Ser335 using a workflow outlined in Figure S3. Briefly, the HEK293T/sASBT cells were grown in triplicate and then treated with 0.1% DMSO as the vehicle control or with different kinase inhibitors (all at final concentration of 0.1% DMSO) followed by membrane isolation. After tryptic digestion, peptides from all samples were pooled and spiked with SIL peptides before being analyzed by mass spectrometry to determine the average amount of phosphopeptide and nonphosphopeptide in each batch preparation. After normalizing the peptide amounts, aliquots were spiked with either phosphorylated SIL peptides or nonphosphorylated SIL peptides in a ratio of 1:1 for endogenous/SIL peptides. This method was previously demonstrated to study the phosphorylation stoichiometry of EGFR, and the authors reported that a ratio of about 1:1 to 1:10 between endogenous peptide and spiked-in SIL peptide can be used for accurate quantification.[24] The phosphopeptide aliquots underwent phosphopeptide enrichment before nanoLC-PRM analysis, while the nonphosphorylated peptide fraction was directly analyzed using nanoLC-PRM.

For analyzing the kinase responsible for phosphorylation of Ser335, the kinase inhibitors for PKC, PKA, MEK, MAPK, and CaMKII were chosen based on previous research that suggested the involvement of these kinases in ASBT uptake activity from rat ileum cells, rat kidney tubular cells, and Caco2 cell culture. We used concentrations of these kinase inhibitors which were in the range reported to specifically affect their target kinase activities as reported in these studies.[15,37,38] In

https://doi.org/10.1021/acsomega.4c02999
ACS Omega 2024, 9, 38477−38489

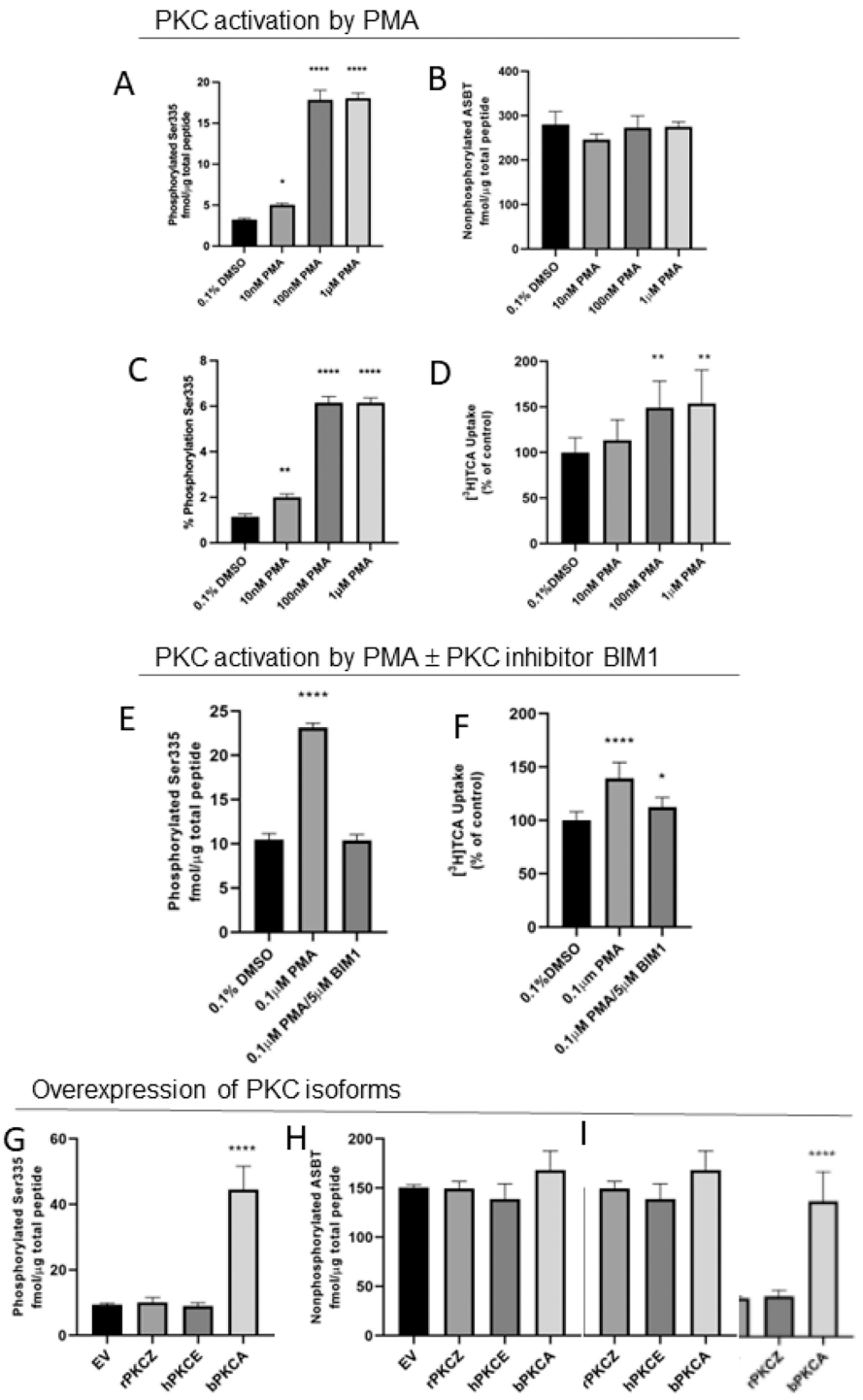

Figure 4. PKC activation or specific isoform overexpression increases ASBT phosphorylation and its TCA uptake activity. PKC activation by PMA (A−D). Amount of Ser335 phosphopeptide (A) and its nonphosphopeptide counterpart (B) were quantified as fmol/μg total peptide based on the known amount of spiked-in stable isotope-labeled peptides; phosphorylation occupancy of Ser335 (C); and TCA uptake assay of ASBT (D) upon treatment with different dose of PMA for 15 min. PKC activation by PMA ± PKC inhibitor BIM1 (E,F). Amount of Ser335 phosphopeptide (E) and TCA uptake assay of ASBT (F) in the presence of 0.1 μM PMA with or without 5 μM BIM1. Overexpression of PKC isoforms (G−I). Amount of phosphorylated Ser335 (G) and its corresponding nonphosphorylated peptide (H), and Ser335 phosphorylation occupancy (I) for empty vector (EV), human PRKCε (hPKCE), rat PRKCζ (rPKCZ), and bovine PRKCα (bPKCA). Uptake of TCA was measured in a 12 min assay using 10 μM cold nonradiolabeled TCA spiked with 1 μCi/mL [^{3}H]-TCA. Uptake assay data are presented as percentage of control. Values are mean ± SD with n = 3 for A,B,C,E, n = 8 for D, n = 12 for F, and n = 2−3 for G,H,I. Significance levels are indicated as follows ****p-value <0.0001, **value <0.007, *p-value <0.03 (Dunnett's post hoc test), indicating statistical significance compared to the control.

addition, we included kinase inhibitors for GRK and CK2 that were predicted to phosphorylate ASBT at the Ser334, Ser335 by NetPhorest 2.1.[39] As shown in Figure 3A, treatment with kinase inhibitors for 6 h significantly reduced Ser335 phosphorylation level, with BIM1 (PKC inhibitor) and H89 (PKA inhibitor) having the greatest inhibitory effects. PKC

https://doi.org/10.1021/acsomega.4c02999
ACS Omega 2024, 9, 38477−38489

and PKA inhibitors reduce Ser335 phosphorylation by 3.95 and 3.45 times, respectively. Inhibitors of GRK, MEK, and MAPK reduced Ser335 phosphorylation by 2.0−2.9 times. CK2 and CaMK II inhibitors have the least effect, with the phosphorylation of Ser335 reduced by 1.4 and 1.7 times, respectively. With the exception of GRK and CaMKII inhibitors, these kinase inhibitors had no significant effect on nonphosphopeptide levels (Figure 3B). The GRK and CaMKII inhibitors reduced the ASBT protein expression at 1.47 and 1.3 times compared to the vehicle control. As a result, the GRK and CaMKII inhibitors may affect protein expression rather than Ser335 phosphorylation. The phosphorylation occupancy of Ser335 reduced from 0.79 to 0.22% and 0.27% upon treatment with PKC and PKA inhibitors which is approximately 3.5 times and 2.9 times decreased in stoichiometry of Ser335 phosphorylation, respectively. Other kinase inhibitors reduced Ser335 phosphorylation occupancy by 1.3 to 2.5 times (Figure 3C). We then examined the effect of these kinase inhibitors on ASBT function using a taurocholate uptake assay and discovered that PKC inhibitor BIM1 has the most significant inhibition effect on ASBT uptake activity (Figure 3D). Other kinase inhibitors had a lesser effect on the ASBT uptake activity compared to the PKC inhibitor. Together these data provide direct evidence using targeted mass spectrometry that the level of ASBT phosphorylation at Ser335 is proportional to ASBT uptake activity and PKC may play a role in regulation of ASBT function and phosphorylation.

Quantification of Phosphosite Occupancy Shows PKC is the Major Kinase Involved in Regulation of ASBT-Ser335 Phosphorylation and ASBT Activity. The PRM methodology for ASBT phosphopeptide quantification described above was further applied to confirm the critical role of PKC in ASBT phosphorylation and function. Cells were treated for 15 min with a specific PKC activator, phorbol 12-myristate 13-acetate (PMA), at three different concentrations (10 nM, 100 nM, and 1 μM) and phosphorylation occupancy of Ser335 was quantified as described above. Indeed, PMA induced phosphorylation of ASBT at Ser335 in a dose-dependent manner, while having no effect on the amount of nonphosphorylated peptide (Figure 4A,B). Phosphorylation of Ser335 increases 1.6, 5.5, and 5.6 times at 10 nM, 100 nM, and 1 μM, respectively (Figure 4A). This change in the amount of phosphopeptide also reflects PMA's similar effect on the phosphorylation occupancy of Ser335 over total protein. Ser335 phosphorylation occupancy increased from 1.15 to 2% at 10 nM PMA, and to 6.6% at 100 nM and 1 μM (Figure 4C). Similarly, PMA treatment increases the taurocholate uptake activity of ASBT in a dose-dependent manner (Figure 4D). PKC activation appears to be saturated on both phosphorylation and taurocholate uptake activity of ASBT at 100 nM PMA. Furthermore, we showed that in the presence of the PKC inhibitor BIM1, this activation by PMA were suppressed both in the Ser335 phosphorylation level and the ASBT uptake activity (Figure 4E,F). This result further supports the positive correlation between the Ser335 phosphorylation level and ASBT function. In addition, we compare the activation effect of a PKC activator (PMA) and a PKA activator (forskolin) on the phosphorylation of Ser335. We also included the PKA and PKC inhibitors for comparison. When compared to 10 μM forskolin, the PMA has higher activation effect on ASBT phosphorylation occupancy, increased 11.8 times by PMA vs 2.4 times by forskolin (Figure S4A). The activation by forskolin dropped at 30 μM, indicating that a higher concentration of forskolin might have adverse effects on ASBT phosphorylation. Similarly, PMA has a stronger activation effect on the ASBT bile acid uptake assay compared to forskolin (Figure S4D). This result indicate that PKC is the major kinase regulating the Ser335 phosphorylation and activity of ASBT. We found that the PKC and PKA kinase inhibitors BIM1 and H89 had no significant effect on ASBT phosphorylation after 30 min of treatment. These results suggest that the basal level of Ser335 phosphorylation in ASBT remains relatively stable and that a longer duration of kinase inhibitor treatment is required to observe a decrease in ASBT phosphorylation.

Overexpression of PKCα Increases ASBT Phosphorylation at Ser335. In order to determine which PKC isoforms are involved in the regulation of ASBT phosphorylation, we overexpressed three different PKC isoforms from three different family groups in HEK293T/sASBT and then employed the PRM methodology to quantify phosphorylation occupancy. PKCα is a classic PKC that requires negatively charged phospholipids, diacylglycerol (DAG) or phorbol ester, and calcium for activity; PKCε is a novel PKC that does not require calcium; and PKCζ is an atypical PKC that requires only negatively charged phospholipids for activity. All of these three PKC informs constructs have a FLAG tag and was well-studied by Alex Toker lab.[26−28] The expression of these PKC isoforms was confirmed using Western blot with an anti-FLAG antibody (Figure S5). Interestingly, only PKCα overexpression significantly increases Ser335 phosphorylation, while PKCε and PKCζ have no effect (Figure 4G). PKCα overexpression has no effect on the amount of ASBT nonphosphopeptide counterpart (Figure 4H), indicating that PKCα regulates ASBT phosphorylation but not the ASBT expression level. According to the Western blot results, the expression levels of these kinase isoforms are not significantly different from one another, and thus the increase in phosphorylation of ASBT is due to the effect of PKCα specifically, rather than because PKCα is expressed more than the other two PKC isoforms. It is worth noting that we obtained these isoforms constructs from the same lab and they come from different organisms, but previous research indicates that PKC is highly conserved in animals, so the difference in species source should not affect the outcome.[40] Furthermore, human PKCε did not increase the phosphorylation of Ser335, implying that PKCα plays a regulatory role in controlling ASBT phosphorylation.

DISCUSSION

In this study, we developed a targeted PRM mass spectrometry workflow to identify and quantify the phosphorylation stoichiometry of ASBT and used ligand uptake assays to define the relationship between transporter activity and its phosphorylation state. We unambiguously identified three phosphorylation residues at Thr330, Ser334, and Ser335 based on the specific signature of their b and y ion series and coelution of the endogenous phosphopeptide and its corresponding spiked-in SIL phosphoisoform peptide. We then applied this PRM methodology to characterize the phosphoprofile of a membrane transporter protein using an isolated membrane fraction. The developed PRM method was used to quantify phosphopeptide and nonphosphopeptide abundance in order to determine the phosphorylation site occupancy at specific phosphosites. We then demonstrated the utility of this approach through a series of biologically relevant experiments including identification of the most highly

https://doi.org/10.1021/acsomega.4c02999
ACS Omega 2024, 9, 38477−38489

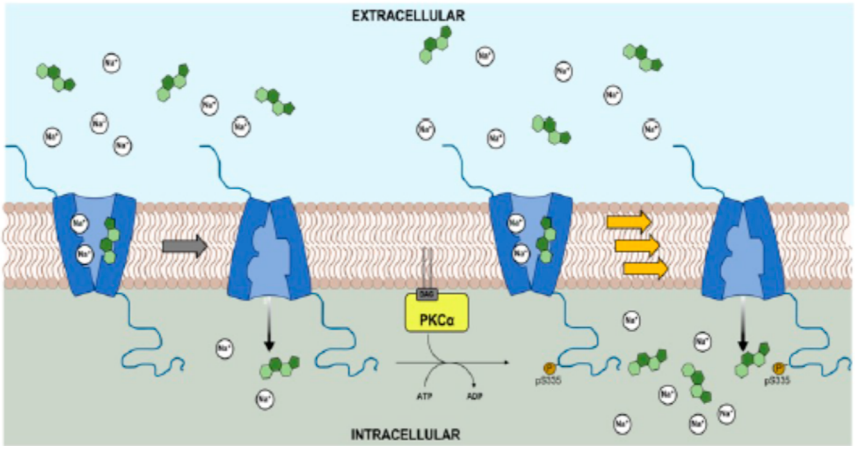

Figure 5. Model for regulation of ASBT activity by phosphorylation at the C-terminal domain. Under basal conditions, ASBT is phosphorylated at Ser 335 by PKC, specifically, the isoform PKCα. Stimulation of PKC activity increases the phosphorylation of Ser 335 and the total activity of ASBT. This is a reversible process because kinase inhibitors reduce the level of phosphorylation at Ser 335 and inhibit its activity.

phosphorylated site (Ser335), the effect of various kinase inhibitors to identify PKC as the kinase most likely responsible for the phosphorylation of Ser335, and the modulation of phosphosite occupancy after various activators, inhibitors, and overexpression. The PRM method is superior when no antibody specific for each phosphoisoform is available as well as when the phosphorylation of the plasma membrane protein is lowly abundant and may be overlooked or excluded by DDA approaches. To the best of our knowledge, this is the first study to identify specific phosphosites of ASBT using mass spectrometry.

The strict evolutionary conservation of Ser335 across mammalian species, including chicken, rat, mouse, rabbit, dog, and human ASBT suggests its biological importance in serine phosphorylation-mediated regulation of ASBT and underpins our observation that it is the major ASBT phosphosite. The effect on Ser335 phosphorylation and ASBT-mediated bile acid absorption of different kinase inhibitors suggests that PKC is the primary kinase that might directly phosphorylate Ser335 and, in turn, regulate ASBT activity. This is supported by the opposing effects of the PKC inhibitor BIM1 and the PKC activator PMA on Ser335 phosphorylation levels and, consequently, ASBT activity (Figures 3 and 4). Furthermore, PMA reveals a more pronounced activation effect compared to the PKA activator forskolin, indicating, again, that PKC is the primary kinase in the regulation of ASBT phosphorylation at Ser335. In addition, the reciprocal effects of a PKC inhibitor that reduced ASBT's Ser335 phosphorylation and its uptake activity, and a PKC activator (PMA) that increased both phosphorylation and ASBT uptake activity, suggests that Ser335 phosphorylation has a positive correlation with the protein's bile acid uptake activity (Figure 5).

Other kinase inhibitors may also regulate ASBT phosphorylation and activity, either directly or by influencing upstream events that eventually affect PKC action. Another possibility is that various kinases are involved under different conditions to tune ASBT activity to different levels required to respond to distinct environments and environmental stimuli during digestion. Because kinase inhibitors and kinase activators typically do not significantly alter protein expression in the total membrane fraction, changes in ASBT activity may, therefore, be due to Ser335 phosphorylation levels. Previous studies used kinase inhibitors or activators to implicate the involvement of phosphorylation regulation of ASBT expression and activity at the cell surface. However, there is no evidence whether these kinases affect the phosphorylation of ASBT and the specific phosphorylation site(s) where ASBT undergoes phosphorylation. As the Strep Tag II system was employed in this study for the initial purification of ASBT to identify phosphorylation sites, it was not feasible to concurrently perform surface expression assays with the same system. Future investigations that integrate both phosphoproteomics and quantification of ASBT surface expression would be beneficial in determining whether phosphorylation impacts ASBT expression at the cell surface. Furthermore, the collective findings are contradictory; some studies found that kinase inhibitors suppress ASBT uptake activity, whereas others suggest that ASBT kinase activators inhibit ASBT activity.[14−16,37,41,42] As a result, there is no conclusive evidence that these kinase inhibitors and activators indeed change ASBT phosphorylation levels and thus regulate the uptake activity. It should be noted that the different results in all of the studies cited can be due to the difference in regulation of ASBT in distinct cell types, such as the kidney, intestine, or bile duct. Future research could use PRM mass spectrometry to investigate the phosphorylation of ASBT in vivo in ileocytes, cholangiocytes, or renal tubular cells to gain a better understanding whether the ASBT phosphorylation differs between organs. Another possibility is that the time of treatment and the status of the cells when treated, such as whether or not the cells were starved prior to treatment, as well as the control used for comparing the kinase inhibitors and activators on ASBT uptake activity, may influence the outcome. Here, we dissolved all of the chemicals in DMSO and treated the cells at a final concentration of 0.1% DMSO; accordingly, we used DMSO 0.1% as the vehicle control, whereas other studies may have used an inactive analog of the kinase inhibitor/activator as control. Schlattjan and co-workers found that both inactive form (KN92) and active form (KN93) have similar inhibitory effect on ASBT uptake activity when compared to the DMSO vehicle control,[38] indicating that the control factor used to normalize the ASBT function must be considered.

PKC is a Ca^{2+}-activated, phospholipid-dependent phosphorylase that is important for membrane signal transduction and

https://doi.org/10.1021/acsomega.4c02999
ACS Omega 2024, 9, 38477−38489

has a significant effect on intestinal epithelial functions.[43] For example, the divalent metal transporter DMT1 (also known as Nramp2 or SLC11A2) shuttles iron across the intestinal mucosa and is phosphorylated at Ser43 under basal conditions, as detected by phosphoserine antibody. Treatment of DMT1-expressing cells with staurosporine—a broad spectrum inhibitor of PKA and PKC— inhibits DMT1 phosphorylation and thus inhibits iron uptake activity in these cells.[44] Previously, Edman sequencing was used to identify multiple serine phosphosites of P-glycoprotein (P-gp), and PKC was found to regulate P-gp phosphorylation.[45,46] In the present study, PKCα is shown to be a major isoform that regulates the phosphorylation of Ser335 ASBT. Interestingly, bile acids such as taurocholate and tauroursodeoxycholate activate PKCα in cultured rat hepatocytes within 15 min of treatment,[47,48] implying that PKCα plays an important role in the rapid regulation of ASBT phosphorylation and may be involved in a feedback loop. Future work will need to clearly establish a discrete molecular basis of the correlation between the bile acid uptake activity and phosphorylation level of ASBT.

Finally, our findings present a straightforward mass spectrometry workflow for quantifying ASBT phosphorylation and ASBT expression from total membrane protein fractions without the need for protein purification, which could require a large amount of material. As a result, our method can be applied under a variety of conditions. For example, we can use a similar workflow to identify the phosphatase that regulates ASBT dephosphorylation. We can also use the method to examine the phophorylation level of ASBT after treatment with various ASBT-targeting compounds used to treat diseases such as hypercholesterolemia, cholestasis, and type 2 diabetes.[6] This is especially useful in light of recent clinical advances in the use of ASBT inhibitors.

■ ASSOCIATED CONTENT

Data Availability Statement

All untargeted and targeted proteomics data and raw files are available through Panorama repository[31] under the data set identifier PXD035472[32] and via https://panoramaweb.org/asbt.url.

Supporting Information

The Supporting Information is available free of charge at https://pubs.acs.org/doi/10.1021/acsomega.4c02999.

Expression and in vivo activity of Strep II-tagged apical sodium-dependent bile acid transporter (sASBT) in transfected cell lines, the conservation of serine 335 across vertebrates, the workflow for quantifying the phoshporylation stoichiometry of ASBT, the effect of PKC stimulation on the phosphorylation of Ser335 as compared to stimulation of PKA, and the overexpression of PKC isoforms is included (PDF)

The data exported from Skyline for quantification of phosphopeptide at Ser335 and its corresponding non-phosphopeptide is also provided (XLSX)

■ AUTHOR INFORMATION

Corresponding Authors

Maureen A. Kane − *Department of Pharmaceutical Sciences, University of Maryland School of Pharmacy, Baltimore, Maryland 21201, United States;* orcid.org/0000-0002-5525-9170; Email: mkane@rx.umaryland.edu

Peter W. Swaan − *Department of Pharmaceutical Sciences, University of Maryland School of Pharmacy, Baltimore, Maryland 21201, United States;* Present Address: Department of Pharmaceutics University of Florida College of Pharmacy Gainesville, FL 32608. Email: peter.swaan@ufl.edu; orcid.org/0000-0003-1767-1487; Email: pswaan@rx.umaryland.edu

Author

Thao T. Nguyen − *Department of Pharmaceutical Sciences, University of Maryland School of Pharmacy, Baltimore, Maryland 21201, United States;* Present Address: Gehrke Proteomics Center Christopher S. Bond Life Sciences Center University of Missouri Columbia, MO 65211.; orcid.org/0000-0003-3877-3220

Complete contact information is available at: https://pubs.acs.org/10.1021/acsomega.4c02999

Notes

The authors declare no competing financial interest.

■ ACKNOWLEDGMENTS

This work was supported in part by R01DK61425 (to P.W.S.) from the National Institute of Diabetes and Digestive and Kidney Diseases (NIDDK) and by the University of Maryland Baltimore, School of Pharmacy Mass Spectrometry Center (SOP1841-IQB2014). The authors would like to express thanks to Dr. Ebehiremen Ayewoh for assistance with cell culture and the bile acid uptake assay and to Matthew R. Blackburn for his critical review and revision of this manuscript.

■ ABBREVIATIONS

ASBT	apical sodium-dependent bile acid transporter (or SLC10A2)
DMT1	divalent metal transporter 1
P-gp	P-glycoprotein
HNF1-α	hepatocyte nuclear factor 1 alpha
CDX1/2	Caudal-Type Homeobox Transcription Factor 1/2
GATA4	GATA-binding protein 4
RXR	retinoid X receptor
GR	glucocorticoid receptor
GRK	G-protein coupled receptor kinase
DAG	diacylglycerol
cAMP	cyclic adenosine monophosphate
IL1β	interleukin 1 beta
PKC	protein kinase C
PKA	protein kinase A
MEK1/2	mitogen-activated protein kinase 1/2
PTMs	post-translational modifications
BCA assay	bicinchoninic acid assay (protein quantification assay)
TCEP	tris(2-carboxyethyl)phosphine
IAA	iodoacetamide
DTT	dithiothreitol
TFA	trifluoroacetic acid
PEPotec	peptide synthesis grade
AQUA	absolute quantification
EPEC	enteropathogenic *Escherichia coli*
COS-1	monkey kidney fibroblast-like cell line
DDA	data dependent acquisition
SRM	selected reaction monitoring

PRM	parallel reaction monitoring
QqQ	Tandem quadrupole
Q-Exactive	quadrupole-Orbitrap
Fusion Tribrid	quadrupole-Orbitrap-linear ion trap
QqTOF	quadrupole/time-of-flight
MS/MS	Tandem mass spectrometry
nanoLC-MS/MS	nano liquid chromatography-tandem mass spectrometry
KN-93	calcium/calmodulin-dependent protein kinase II inhibitor
CCG215022	PKA kinase inhibitor
U0126	MEK inhibitor
SB203580	p38 MAPK inhibitor
CMPD101	kinase inhibitor
FSK	PKA activators forskolin
IBMX	3-isobutyl-1-methylxanthine
PMA	phorbol 12-myristate 13-acetate
MBCD	methyl-β-cyclodextrin
SDS	sodium dodecyl sulfate
DDM	*n*-dodecyl-β-D-maltopyranoside
Opti-MEM	optimized minimum essential medium
WT	wild-type

REFERENCES

(1) Hagenbuch, B.; Dawson, P. The sodium bile salt cotransport family SLC10. *Pflugers Arch.* **2004**, *447* (5), 566−570.

(2) Weinman, S. A.; Carruth, M. W.; Dawson, P. A. Bile acid uptake via the human apical sodium-bile acid cotransporter is electrogenic. *J. Biol. Chem.* **1998**, *273* (52), 34691−34695.

(3) Claro da Silva, T.; Polli, J. E.; Swaan, P. W. The solute carrier family 10 (SLC10): beyond bile acid transport. *Mol. Aspects Med.* **2013**, *34* (2−3), 252−269.

(4) Anwer, M. S.; Stieger, B. Sodium-dependent bile salt transporters of the SLC10A transporter family: more than solute transporters. *Pflugers Arch.* **2014**, *466* (1), 77−89.

(5) Xiao, L.; Pan, G. An important intestinal transporter that regulates the enterohepatic circulation of bile acids and cholesterol homeostasis: The apical sodium-dependent bile acid transporter (SLC10A2/ASBT). *Clin. Res. Hepatol. Gastroenterol.* **2017**, *41* (5), 509−515.

(6) Yang, N.; Dong, Y. Q.; Jia, G. X.; Fan, S. M.; Li, S. Z.; Yang, S. S.; Li, Y. B. ASBT(SLC10A2): A promising target for treatment of diseases and drug discovery. *Biomed. Pharmacother.* **2020**, *132*, 110835.

(7) Li, M.; Wang, Q.; Li, Y.; Cao, S.; Zhang, Y.; Wang, Z.; Liu, G.; Li, J.; Gu, B. Apical sodium-dependent bile acid transporter, drug target for bile acid related diseases and delivery target for prodrugs: Current and future challenges. *Pharmacol. Ther.* **2020**, *212*, 107539.

(8) Annaba, F.; Sarwar, Z.; Kumar, P.; Saksena, S.; Turner, J. R.; Dudeja, P. K.; Gill, R. K.; Alrefai, W. A. Modulation of ileal bile acid transporter (ASBT) activity by depletion of plasma membrane cholesterol: association with lipid rafts. *Am. J. Physiol. Gastrointest. Liver Physiol.* **2008**, *294* (2), G489−G497.

(9) Ticho, A. L.; Malhotra, P.; Manzella, C. R.; Dudeja, P. K.; Saksena, S.; Gill, R. K.; Alrefai, W. A. S-acylation modulates the function of the apical sodium-dependent bile acid transporter in human cells. *J. Biol. Chem.* **2020**, *295* (14), 4488−4497.

(10) Ayewoh, E. N.; Czuba, L. C.; Nguyen, T. T.; Swaan, P. W. S-acylation status of bile acid transporter hASBT regulates its function, metabolic stability, membrane expression, and phosphorylation state. *Biochim. Biophys. Acta Biomembr.* **2021**, *1863* (2), 183510.

(11) Zhang, E. Y.; Phelps, M. A.; Banerjee, A.; Khantwal, C. M.; Chang, C.; Helsper, F.; Swaan, P. W. Topology scanning and putative three-dimensional structure of the extracellular binding domains of the apical sodium-dependent bile acid transporter (SLC10A2). *Biochemistry* **2004**, *43* (36), 11380−11392.

(12) Muthusamy, S.; Malhotra, P.; Hosameddin, M.; Dudeja, A. K.; Borthakur, S.; Saksena, S.; Gill, R. K.; Dudeja, P. K.; Alrefai, W. A. N-glycosylation is essential for ileal ASBT function and protection against proteases. *Am. J. Physiol. Cell Physiol.* **2015**, *308* (12), C964−C971.

(13) Xia, X.; Roundtree, M.; Merikhi, A.; Lu, X.; Shentu, S.; Lesage, G. Degradation of the apical sodium-dependent bile acid transporter by the ubiquitin-proteasome pathway in cholangiocytes. *J. Biol. Chem.* **2004**, *279* (43), 44931−44937.

(14) Schlattjan, J. H.; Benger, S.; Herrler, A.; von Rango, U.; Greven, J. Regulation of taurocholate transport in freshly isolated proximal tubular cells of the rat kidney by protein kinases. *Nephron. Physiol.* **2005**, *99* (2), p35−p42.

(15) Sarwar, Z.; Annaba, F.; Dwivedi, A.; Saksena, S.; Gill, R. K.; Alrefai, W. A. Modulation of ileal apical Na+-dependent bile acid transporter ASBT by protein kinase C. *Am. J. Physiol. Gastrointest. Liver Physiol.* **2009**, *297* (3), G532−G538.

(16) Al-Hilal, T. A.; Chung, S. W.; Alam, F.; Park, J.; Lee, K. E.; Jeon, H.; Kim, K.; Kwon, I. C.; Kim, I. S.; Kim, S. Y.; Byun, Y. Functional transformations of bile acid transporters induced by high-affinity macromolecules. *Sci. Rep.* **2014**, *4*, 4163.

(17) Annaba, F.; Sarwar, Z.; Gill, R. K.; Ghosh, A.; Saksena, S.; Borthakur, A.; Hecht, G. A.; Dudeja, P. K.; Alrefai, W. A. Enteropathogenic Escherichia coli inhibits ileal sodium-dependent bile acid transporter ASBT. *Am. J. Physiol. Gastrointest. Liver Physiol.* **2012**, *302* (10), G1216−G1222.

(18) Chothe, P. P.; Czuba, L. C.; Ayewoh, E. N.; Swaan, P. W. Tyrosine Phosphorylation Regulates Plasma Membrane Expression and Stability of the Human Bile Acid Transporter ASBT (SLC10A2). *Mol. Pharm.* **2019**, *16* (8), 3569−3576.

(19) Orsburn, B. C.; Stockwin, L. H.; Newton, D. L. Challenges in plasma membrane phosphoproteomics. *Expert Rev. Proteomics* **2011**, *8* (4), 483−494.

(20) Lange, V.; Picotti, P.; Domon, B.; Aebersold, R. Selected reaction monitoring for quantitative proteomics: a tutorial. *Mol. Syst. Biol.* **2008**, *4*, 222.

(21) Gallien, S.; Duriez, E.; Crone, C.; Kellmann, M.; Moehring, T.; Domon, B. Targeted proteomic quantification on quadrupole-orbitrap mass spectrometer. *Mol. Cell. Proteomics* **2012**, *11* (12), 1709−1723.

(22) Peterson, A. C.; Russell, J. D.; Bailey, D. J.; Westphall, M. S.; Coon, J. J. Parallel reaction monitoring for high resolution and high mass accuracy quantitative, targeted proteomics. *Mol. Cell. Proteomics* **2012**, *11* (11), 1475−1488.

(23) Schilling, B.; MacLean, B.; Held, J. M.; Sahu, A. K.; Rardin, M. J.; Sorensen, D. J.; Peters, T.; Wolfe, A. J.; Hunter, C. L.; MacCoss, M. J.; Gibson, B. W. Multiplexed, Scheduled, High-Resolution Parallel Reaction Monitoring on a Full Scan QqTOF Instrument with Integrated Data-Dependent and Targeted Mass Spectrometric Workflows. *Anal. Chem.* **2015**, *87* (20), 10222−10229.

(24) Dekker, L. J. M.; Zeneyedpour, L.; Snoeijers, S.; Joore, J.; Leenstra, S.; Luider, T. M. Determination of Site-Specific Phosphorylation Ratios in Proteins with Targeted Mass Spectrometry. *J. Proteome Res.* **2018**, *17* (4), 1654−1663.

(25) Campeau, E.; Ruhl, V. E.; Rodier, F.; Smith, C. L.; Rahmberg, B. L.; Fuss, J. O.; Campisi, J.; Yaswen, P.; Cooper, P. K.; Kaufman, P. D. A versatile viral system for expression and depletion of proteins in mammalian cells. *PLoS One* **2009**, *4* (8), No. e6529.

(26) Cenni, V.; Doppler, H.; Sonnenburg, E. D.; Maraldi, N.; Newton, A. C.; Toker, A. Regulation of novel protein kinase C epsilon by phosphorylation. *Biochem. J.* **2002**, *363* (3), 537−545.

(27) Hodges, R. R.; Kazlauskas, A.; Toker, A.; Dartt, D. A. Effect of Overexpression of Protein Kinase Cα on Rat Lacrimal Gland Protein Secretion. *Effect of Overexpression of Protein Kinase Cα on Rat Lacrimal Gland Protein Secretion*; Sullivan, D. A., Stern, M. E., Tsubota, K., Dartt, D. A., Sullivan, R. M., Bromberg, B. B., Eds.; Springer: Boston, MA, 2002; Vol. *506*, pp 237−241.

(28) Chou, M. M.; Hou, W.; Johnson, J.; Graham, L. K.; Lee, M. H.; Chen, C. S.; Newton, A. C.; Schaffhausen, B. S.; Toker, A. Regulation

https://doi.org/10.1021/acsomega.4c02999
ACS Omega 2024, 9, 38477−38489

of protein kinase C zeta by PI 3-kinase and PDK-1. *Curr. Biol.* **1998**, *8* (19), 1069−1078.
(29) Wessel, D.; Flugge, U. I. A method for the quantitative recovery of protein in dilute solution in the presence of detergents and lipids. *Anal. Biochem.* **1984**, *138* (1), 141−143.
(30) MacLean, B.; Tomazela, D. M.; Shulman, N.; Chambers, M.; Finney, G. L.; Frewen, B.; Kern, R.; Tabb, D. L.; Liebler, D. C.; MacCoss, M. J. Skyline: an open source document editor for creating and analyzing targeted proteomics experiments. *Bioinformatics* **2010**, *26* (7), 966−968.
(31) Sharma, V.; Eckels, J.; Taylor, G. K.; Shulman, N. J.; Stergachis, A. B.; Joyner, S. A.; Yan, P.; Whiteaker, J. R.; Halusa, G. N.; Schilling, B.; Gibson, B. W.; Colangelo, C. M.; Paulovich, A. G.; Carr, S. A.; Jaffe, J. D.; MacCoss, M. J.; MacLean, B. Panorama: a targeted proteomics knowledge base. *J. Proteome Res.* **2014**, *13* (9), 4205−4210.
(32) Perez-Riverol, Y.; Csordas, A.; Bai, J.; Bernal-Llinares, M.; Hewapathirana, S.; Kundu, D. J.; Inuganti, A.; Griss, J.; Mayer, G.; Eisenacher, M.; Perez, E.; Uszkoreit, J.; Pfeuffer, J.; Sachsenberg, T.; Yilmaz, S.; Tiwary, S.; Cox, J.; Audain, E.; Walzer, M.; Jarnuczak, A. F.; Ternent, T.; Brazma, A.; Vizcaino, J. A. The PRIDE database and related tools and resources in 2019: improving support for quantification data. *Nucleic Acids Res.* **2019**, *47* (D1), D442−D450.
(33) Schmidt, T. G.; Skerra, A. The Strep-tag system for one-step purification and high-affinity detection or capturing of proteins. *Nat. Protoc.* **2007**, *2* (6), 1528−1535.
(34) Ma, C.; Hao, Z.; Huysmans, G.; Lesiuk, A.; Bullough, P.; Wang, Y.; Bartlam, M.; Phillips, S. E.; Young, J. D.; Goldman, A.; Baldwin, S. A.; Postis, V. L. A Versatile Strategy for Production of Membrane Proteins with Diverse Topologies: Application to Investigation of Bacterial Homologues of Human Divalent Metal Ion and Nucleoside Transporters. *PLoS One* **2015**, *10* (11), No. e0143010.
(35) Nguyen, T. T.; Sabat, G.; Sussman, M. R. In vivo cross-linking supports a head-to-tail mechanism for regulation of the plant plasma membrane P-type H(+)-ATPase. *J. Biol. Chem.* **2018**, *293* (44), 17095−17106.
(36) Sun, A. Q.; Balasubramaniyan, N.; Chen, H.; Shahid, M.; Suchy, F. J. Identification of functionally relevant residues of the rat ileal apical sodium-dependent bile acid cotransporter. *J. Biol. Chem.* **2006**, *281* (24), 16410−16418.
(37) Reymann, A.; Braun, W.; Drobik, C.; Woermann, C. Stimulation of bile acid active transport related to increased mucosal cyclic AMP content in rat ileum in vitro. *Biochim. Biophys. Acta* **1989**, *1011* (2−3), 158−164.
(38) Schlattjan, J. H.; Winter, C.; Greven, J. Regulation of renal tubular bile acid transport in the early phase of an obstructive cholestasis in the rat. *Nephron. Physiol.* **2003**, *95* (3), p49−p56.
(39) Miller, M. L.; Jensen, L. J.; Diella, F.; Jorgensen, C.; Tinti, M.; Li, L.; Hsiung, M.; Parker, S. A.; Bordeaux, J.; Sicheritz-Ponten, T.; Olhovsky, M.; Pasculescu, A.; Alexander, J.; Knapp, S.; Blom, N.; Bork, P.; Li, S.; Cesareni, G.; Pawson, T.; Turk, B. E.; Yaffe, M. B.; Brunak, S.; Linding, R. Linear motif atlas for phosphorylation-dependent signaling. *Sci. Signal.* **2008**, *1* (35), ra2.
(40) Dekker, L. V.; Parker, P. J. Protein kinase C–a question of specificity. *Trends Biochem. Sci.* **1994**, *19* (2), 73−77.
(41) Alpini, G.; Glaser, S.; Robertson, W.; Rodgers, R. E.; Phinizy, J. L.; Lasater, J.; LeSage, G. D. Large but not small intrahepatic bile ducts are involved in secretin-regulated ductal bile secretion. *Am. J. Physiol.* **1997**, *272* (5), G1064−G1074.
(42) Alpini, G.; Glaser, S.; Baiocchi, L.; Francis, H.; Xia, X.; Lesage, G. Secretin activation of the apical Na+-dependent bile acid transporter is associated with cholehepatic shunting in rats. *Hepatology* **2005**, *41* (5), 1037−1045.
(43) Mayati, A.; Moreau, A.; Le Vee, M.; Stieger, B.; Denizot, C.; Parmentier, Y.; Fardel, O. Protein Kinases C-Mediated Regulations of Drug Transporter Activity, Localization and Expression. *Int. J. Mol. Sci.* **2017**, *18* (4), 764.
(44) Seo, Y. A.; Kumara, R.; Wetli, H.; Wessling-Resnick, M. Regulation of divalent metal transporter-1 by serine phosphorylation. *Biochem. J.* **2016**, *473* (22), 4243−4254.
(45) Fine, R. L.; Chambers, T. C.; Sachs, C. W. P-glycoprotein, multidrug resistance and protein kinase C. *Stem Cell.* **1996**, *14* (1), 47−55.
(46) Chambers, T. C.; Pohl, J.; Raynor, R. L.; Kuo, J. F. Identification of specific sites in human P-glycoprotein phosphorylated by protein kinase C. *J. Biol. Chem.* **1993**, *268* (7), 4592−4595.
(47) Rao, Y. P.; Stravitz, R. T.; Vlahcevic, Z. R.; Gurley, E. C.; Sando, J. J.; Hylemon, P. B. Activation of protein kinase C alpha and delta by bile acids: correlation with bile acid structure and diacylglycerol formation. *J. Lipid Res.* **1997**, *38* (12), 2446−2454.
(48) Stravitz, R. T.; Rao, Y. P.; Vlahcevic, Z. R.; Gurley, E. C.; Jarvis, W. D.; Hylemon, P. B. Hepatocellular protein kinase C activation by bile acids: implications for regulation of cholesterol 7 alpha-hydroxylase. *Am. J. Physiol.* **1996**, *271* (2), G293−G303.

https://doi.org/10.1021/acsomega.4c02999
ACS Omega 2024, 9, 38477−38489